

A GENERALIZED CORRELATION OF CRITICAL HEAT FLUX FOR THE FORCED CONVECTION BOILING IN VERTICAL UNIFORMLY HEATED ROUND TUBES—A SUPPLEMENTARY REPORT

Y. KATTO

Department of Mechanical Engineering, University of Tokyo,
 Hongo, Bunkyo-ku, Tokyo, Japan

(Received 10 May 1978)

Abstract—Through the comparison with the prediction of a generalized correlation which was developed by the author in the preceding study, the existing data of critical heat flux (CHF) obtained in recent studies, including Milan reproducibility tests and others, are analyzed in the present paper. As the result, not only new information is obtained for the general structure of CHF, but also it is confirmed that the above-mentioned correlation is available as a tool for unifying experiments of various kinds. Besides, the propriety of dimensionless groups with which the generalized correlation is composed is also tested by comparing the prediction of mass flux scaling factor with empirical values obtained in the study of CHF modeling.

NOMENCLATURE

d ,	I.D. of heated tube [m];
F_G ,	mass flux scaling factor;
G ,	mass velocity [$\text{kg}/\text{m}^2 \text{ s}$];
H_{fg} ,	latent heat of evaporation [J/kg];
ΔH_i ,	enthalpy of inlet subcooling [J/kg];
K ,	parameter for inlet subcooling effect, equation (6);
l ,	length of heated tube [m];
p ,	absolute pressure [bar];
q_{c0} ,	critical heat flux [W/m^2];
q_{c0} ,	q_c for $\Delta H_i = 0$ [W/m^2].

Greek symbols

μ_l ,	viscosity of liquid [Ns/m^2];
μ_v ,	viscosity of vapor [Ns/m^2];
ρ_l ,	density of liquid [kg/m^3];
ρ_v ,	density of vapor [kg/m^3];
σ ,	surface tension [N/m];
χ_{ex} ,	exit quality;
$\chi_{ex,0}$,	χ_{ex} for $\Delta H_i = 0$.

1. INTRODUCTION

AMONG recent experimental studies made on the critical heat flux (CHF) of forced convection boiling in vertical uniformly heated round tubes, one should not forget to refer to the study carried out in European laboratories in order to test the reproducibility of CHF data of water providing the Milan reproducibility tests data [1] which may be regarded as very reliable. On the other hand, Becker [2] and Becker and Ling [3] conducted the experiment on CHF of water for two particular cases of a small diameter tube and a tube having a great length. Cumo *et al.* [4] made a comparison of upflow and downflow CHF for Freon-12, Groeneveld [5] conducted an experiment on Freon-12 studying upstream CHF under the condition of not only negative

but also positive quality at the inlet, and Campolunghi *et al.* [6] showed experimental results of water indicating a rapid change of CHF in the interval of pressure from 90 to 110 bars. As for investigations of pure fluids other than water and Freons, Alad'yev *et al.* [7] reported CHF data for potassium, and Pokhvalov *et al.* [8] obtained CHF data for benzene. Considerable progress was also achieved in the study of CHF modeling by Ahmad [9] and others. Unfortunately, however, it seems likely that many important studies such as mentioned above have been left separate and accordingly the mutual relations are not necessarily clear.

Recently, the author [10] developed a generalized correlation of CHF for the forced convection boiling in vertical uniformly heated round tubes. Being compared with the prediction of this correlation, in the present paper, the above-mentioned experimental data plus the data of Freon-22 [21] and Freon-11 [23] are analyzed in order to investigate the general structure of CHF, and at the same time, to test the applicability of the correlation.

2. CORRELATION EQUATIONS OF CHF

2.1. Correlation equations of CHF

From the generalized correlation developed by the author [10], equations necessary in the present paper are abstracted as follows:

First, for prediction of critical heat flux q_{c0} at $\Delta H_i = 0$, L-regime:

$$\frac{q_{c0}}{GH_{fg}} = C \left(\frac{\sigma \rho_l}{G^2 l} \right)^{0.043} \frac{1}{l/d} \quad (1)$$

where C is a constant, 0.25 or 0.34 depending on the conditions.

H-regime:

$$\frac{q_{c0}}{GH_{fg}} = 0.10 \left(\frac{\rho_v}{\rho_l} \right)^{0.133} \left(\frac{\sigma \rho_l}{G^2 l} \right)^{1/3} \frac{1}{1 + 0.0031 l/d} \quad (2)$$

H- and N- regime:

$$\frac{q_{c0}}{GH_{fg}} = 0.098 \left(\frac{\rho_v}{\rho_l} \right)^{0.133} \left(\frac{\sigma \rho_l}{G^2 l} \right)^{0.433} \times \frac{(l/d)^{0.27}}{1 + 0.0031 l/d} \quad (3)$$

HP-regime:

$$\frac{q_{c0}}{GH_{fg}} = 8.20 \left(\frac{\rho_v}{\rho_l} \right)^{0.65} \left(\frac{\sigma \rho_l}{G^2 l} \right)^{0.453} \times \frac{1}{1 + 107 \left(\frac{\sigma \rho_l}{G^2 l} \right)^{0.54} \frac{l}{d}} \quad (4)$$

With respect to equation (3), the boundary between H- and N-regime can be determined by

$$\frac{\sigma \rho_l}{G^2 l} = \left(\frac{0.77}{l/d} \right)^{2.70} \quad (5)$$

Next, in case of $\Delta H_i > 0$, the critical heat flux q_c exhibits the characteristic change such as shown in the region of $\Delta H_i > 0$ in Fig. 1, and for L-, H-, and HP-regime where the linear $q_c - \Delta H_i$ relationship holds, q_c can be predicted by

$$q_c = q_{c0} (1 + K \Delta H_i / H_{fg}) \quad (6)$$

where q_{c0} is given by equations (2)–(4), and K is given as follows:

$$K \text{ in L-regime: } K_L = 1 \quad (7)$$

K in H-regime:

for $\sigma \rho_l / G^2 l < 3 \times 10^{-6}$,

$$K_H = 1.8 \left(\frac{130}{l/d} \right)^{5\rho_v/\rho_l} \quad (8)$$

for $3 \times 10^{-6} < \sigma \rho_l / G^2 l$,

$$K_H = 0.075 \left(\frac{130}{l/d} \right)^{5\rho_v/\rho_l} \left(\frac{\sigma \rho_l}{G^2 l} \right)^{-1/4}$$

K in HP-regime:

for $\sigma \rho_l / G^2 l < 4 \times 10^{-8}$,

$$K_{HP} = 0.664 (\rho_v / \rho_l)^{-0.6} \quad (9)$$

for $4 \times 10^{-8} < \sigma \rho_l / G^2 l$,

$$K_{HP} = 3.08 (\sigma \rho_l / G^2 l)^{0.09} (\rho_v / \rho_l)^{-0.6}.$$

2.2. On the exit quality at CHF for $\Delta H_i = 0$

When $\Delta H_i = 0$, the heat flux q_{c0} is related to the exit quality $\chi_{ex,0}$ via the heat balance, thus,

$$\chi_{ex,0} = 4(q_{c0} / GH_{fg}) l / d \quad (10)$$

q_{c0} / GH_{fg} on the RHS of equation (10) is given by equations (1)–(4), and Fig. 2 shows the result in case of $l/d = 200$ as an example. From Fig. 2, tentative postulation of flow structure at CHF may be made as follows: the annular flow closely allied to dispersed flow in L-regime, where the deficiency of liquid on the heated surface may be responsible for

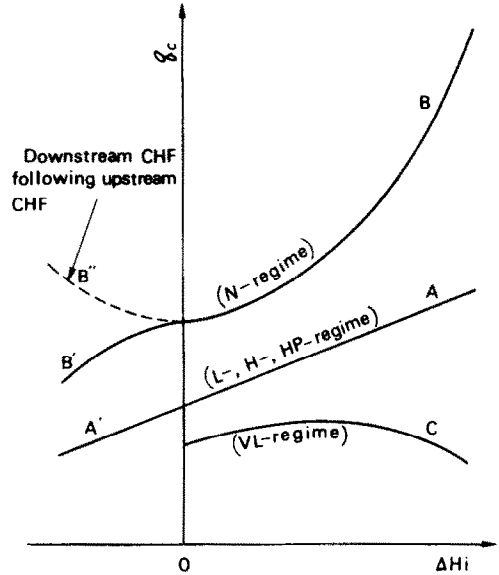


FIG. 1. Relationship between q_c and ΔH_i .

CHF; the annular flow in H-regime, where the hydrodynamic instability of interface may lead to CHF; and the bubble flow in N-regime, where CHF may occur by the transition from nucleate boiling to film boiling. As for HP-regime, the flow structure remains rather vague to the author. However, since the study of CHF mechanism is not the objective of the present paper, the author will only refer to the investigations such as made by Bennett *et al.* [11], Whalley *et al.* [12], Nevstrueva [13], and others which contribute to the understanding of CHF mechanism.

3. L-REGIME

3.1. Comparison with Milan reproducibility tests and particular cases data.

With respect to CHF in L-regime, Fig. 3 shows the comparison of equation (1) with the Milan reproducibility tests data of water (N.B. the data used by Becker *et al.* [14] to compare with various empirical correlations have been displayed in Fig. 3), the water data of Becker [2] for a small diameter tube ($d = 3.0$ mm), and the water data of Becker and Ling [3] for a very long tube ($l = 7.1$ m), on condition that q_{c0} data shown in Fig. 3 are those derived from the original data (q_c vs ΔH_i) through equations (6) and (7). It may be noted in Fig. 3 that CHF occurs at the state $\chi_{ex,0} = 1$ shown by the broken line in Fig. 3 in case of the very long tubes, whereas all the other data agree well with the prediction of equation (1). One point, however, should be checked, because the constant C in equation (1) has been determined in the author's preceding paper [10] as $C = 0.34$ for Freons and $C = 0.25$ for the other fluids, but by contrast in Fig. 3, $C = 0.34$ adapts for water.

Then Fig. 4 is prepared to examine the data of q_{c0} in L-regime derived through equations (6) and (7) from the experimental data compiled or presented by Thomson and Macbeth (Tables 1–10) [15] for water,

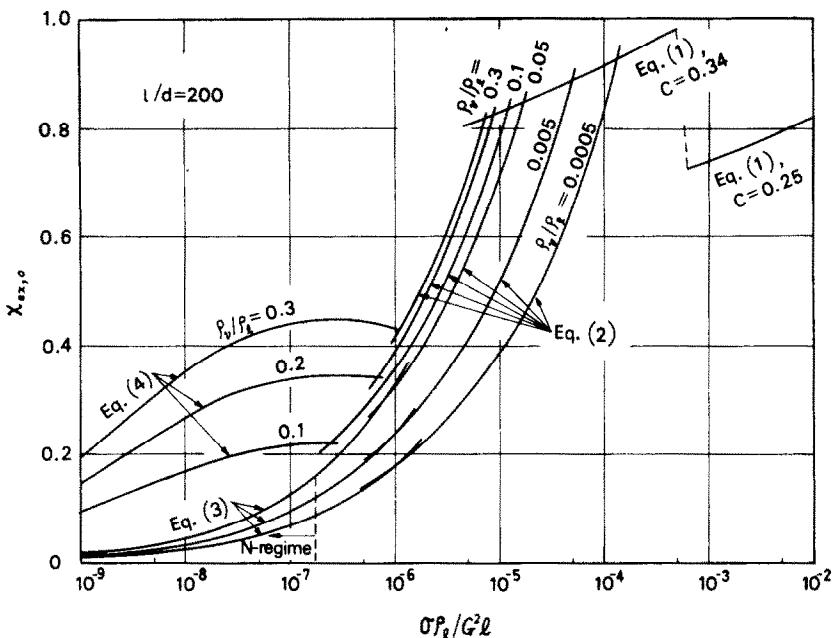


FIG. 2. Exit quality $\chi_{ex,0}$ in case of $\Delta H_i = 0$ and $l/d = 200$.

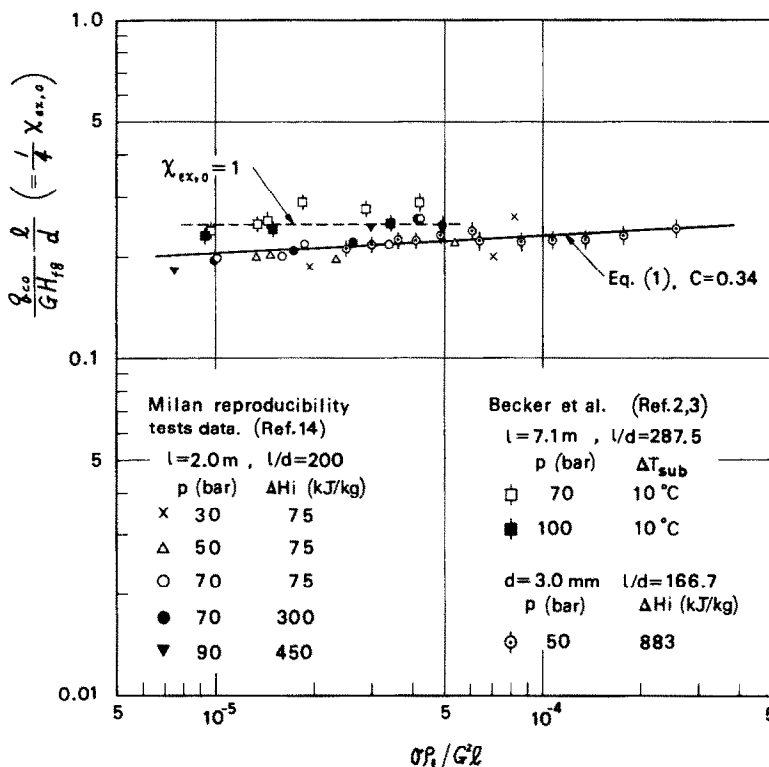


FIG. 3. Comparison between water data in L-regime and the prediction of equation (1).

Lewis *et al.* [16] for liquid hydrogen and nitrogen, Stevens *et al.* [17] for Freon-12 and Barnett *et al.* [18] for Freon-12 and -21. It may be noticed from Figs. 3 and 4 that the value of C seems to change in the vicinity of $\sigma\rho_l/G^2l = 5 \times 10^{-4}$ independently of the kind of fluid. In the author's preceding study [10] having no already-known information for K in equation (6), q_{c0} had to be derived by means of the

extrapolation of q_c as $\Delta H_i \rightarrow 0$ along experimental curves such as shown in Fig. 1, and accordingly the available data of q_{c0} was so limited as to accidentally yield the result that the region of $\sigma\rho_l/G^2l < 5 \times 10^{-4}$ was occupied by the data of Freons alone, erroneously leading to the conclusion that $C = 0.34$ for Freons.

In sum, as for CHF in L-regime, there are usually

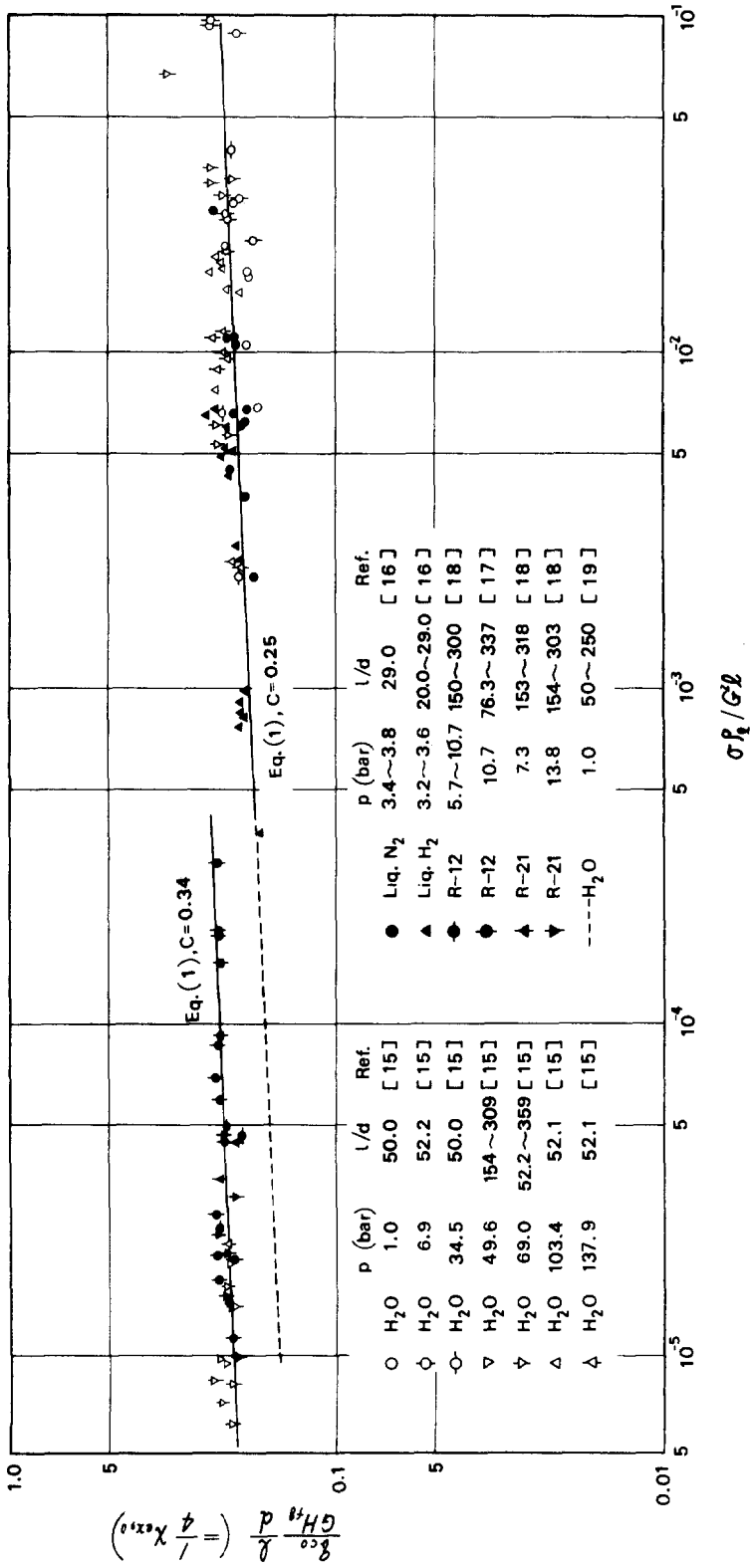


FIG. 4. Experimental data in L-regime and the constant C in equation (1).

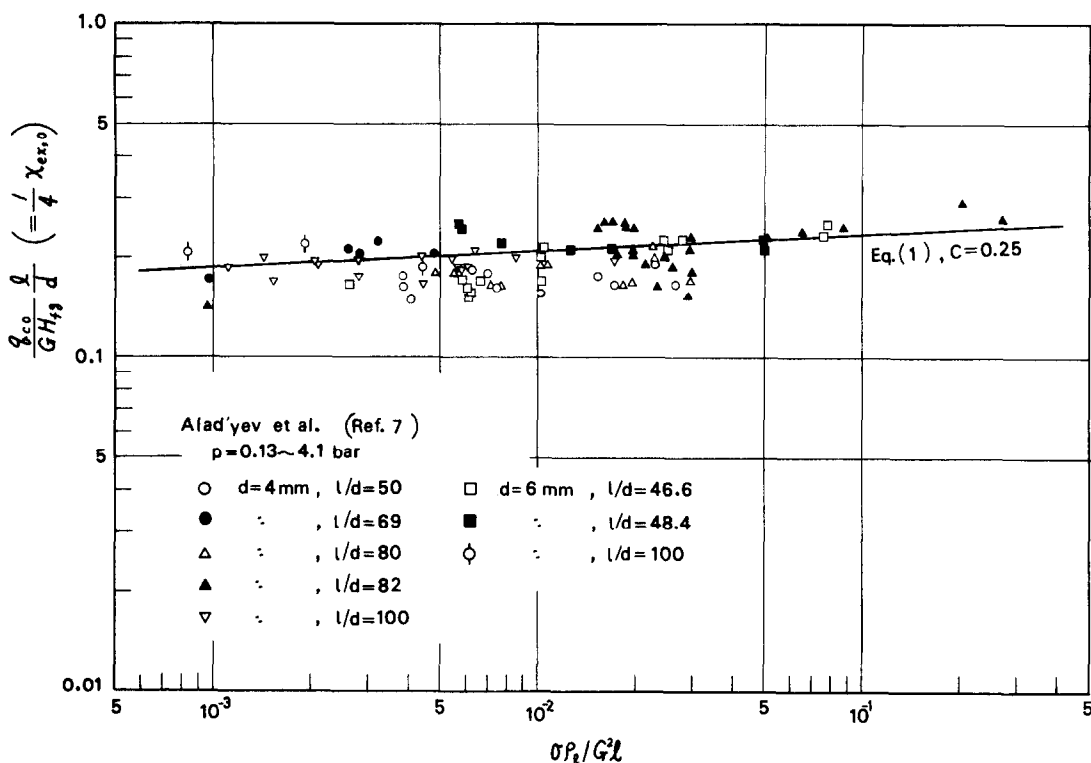


FIG. 5. Comparison between potassium data in L-regime and the prediction of equation (1).

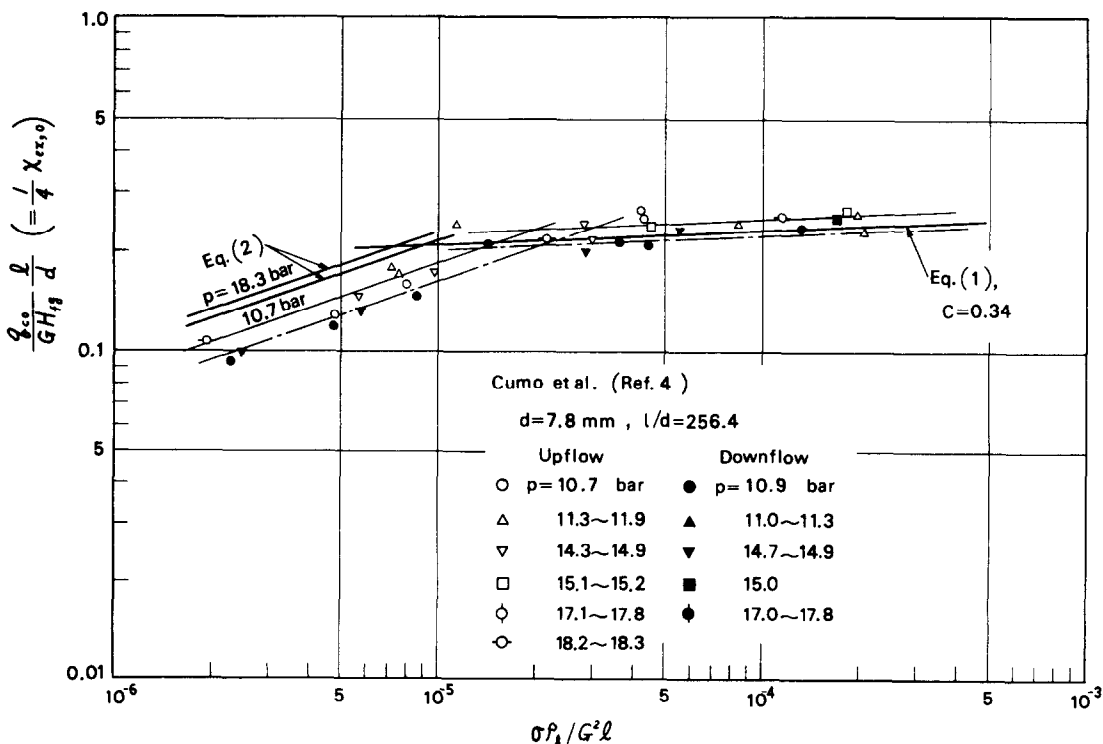


FIG. 6. Upflow and downflow data of Freon-12 in L- and H-regime with the prediction of equations (1), (2) and (5).

two regions of $\sigma\rho_l/G^2l$ characterized by $C = 0.25$ and 0.34 , but in the special case of tubes with great length, $\chi_{ex}=1$ may be the criterion for the onset of CHF. It should be noted, however, that a great many data of water at atmospheric pressure ($d = 1.3-4.8$ mm, $l/d = 50-250$) obtained by Lowdermilk *et al.* (Table III) [19] show the result which adapts to $C = 0.25$ over the whole range of $\sigma\rho_l/G^2l$ in Fig. 4 (see the broken line in Fig. 4). Therefore, further study is still necessary at least before giving the final conclusion for the characteristics of CHF in L-regime.

3.2. Comparison with potassium data

Figure 5 shows the comparison of equation (1) with q_{c0} data derived through equations (6) and (7) from the experimental data of Arad'yev *et al.* [7] for potassium ($p = 0.13-4.1$ bars). As for the surface tension of potassium used to prepare Fig. 5, the experimental data obtained by Kiriyenko (Table 2) [20] at the boundary with potassium vapor has been employed. In addition, the data for $l/d = 30$ have been excluded from the display in Fig. 5, because they were obtained with the conditions including low inlet velocities less than 0.3 m/s, belonging to VL-regime (cf. [10]).

The data in Fig. 5 may be regarded to agree with equation (1) with $C = 0.25$ though some data lie a little lower, and it may be of interest to note that this result is properly in accord with the criterion for CHF determined in the preceding section for the range of $\sigma\rho_l/G^2l > 5 \times 10^{-4}$.

3.3. Comparison between upflow and downflow data

Figure 6 shows the comparison of equation (1) with q_{c0} data which can be obtained by means of the extrapolation of q_c as $\Delta H_i \rightarrow 0$ from the experimental data of Cumo *et al.* [4] for Freon-12. The experimental range is in $\sigma\rho_l/G^2l < 5 \times 10^{-4}$ and it is noted that the data belonging to L-regime show a fairly good agreement with equation (1) with $C = 0.34$ on condition that q_{c0} for upflow is about 11% higher than q_{c0} for downflow. It may not be useless to note that the above data in L-regime are under the condition that $G = 120$ to 325 kg/m²s and $l/d = 256.4$.

4. H-REGIME

4.1. Comparison with Milan reproducibility tests data

With respect to H-regime, Fig. 7 shows the comparison of equations (2) and (3) with q_{c0} data derived through equations (6) and (8) from the Milan reproducibility tests data of water (N.B. the data used by Becker *et al.* [14] have been displayed in Fig. 7). The vertical broken line in Fig. 7 represents the boundary of H- and N-regime predicted by equation (5). The agreement between the data and equations (2) and (3) is fairly good in spite of the difference of pressure as much as three times. If necessary, much better agreement can be realized by a slight modification of constants on the RHS of equations (2) and (3).

4.2. Comparison with particular cases

Figure 8 shows the comparison of equations (2) and (3) with q_{c0} data derived through equations (6)

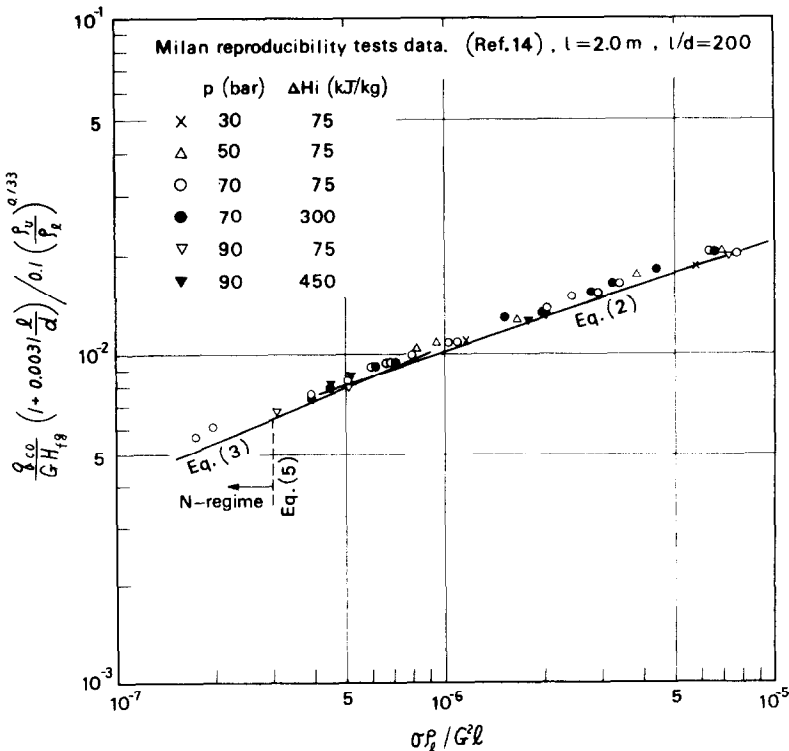


FIG. 7. Comparison between water data in H-regime and the prediction of equations (2), (3) and (5).

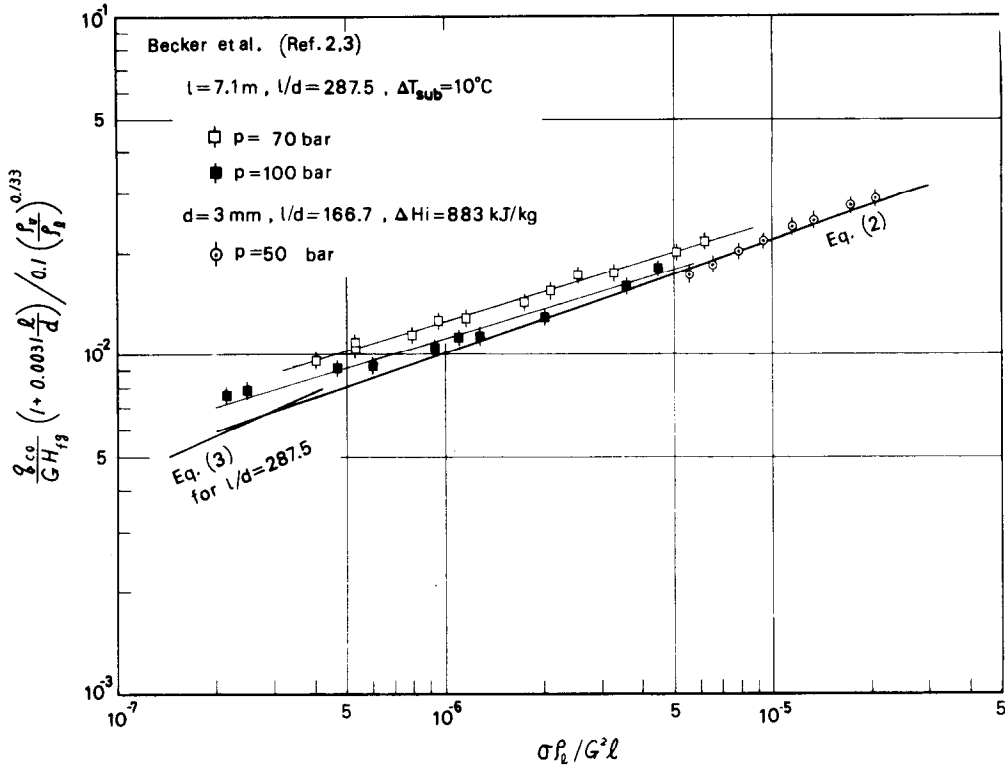


FIG. 8. Comparison between water data in H-regime and the prediction of equations (2) and (3).

and (8) from the experimental data of water in H-regime obtained by Becker [2] and Becker and Ling [3] for two particular cases of $d = 3$ mm and $l = 7.1$ m. The data for $d = 3$ mm show a good agreement with equation (2), whereas the data for the tube having a great length not only lie slightly higher than equation (2) but also show the variation of q_{c0}/GH_{fg} in proportion to $(\sigma\rho_l/G^2l)^{0.29}$ instead of $(\sigma\rho_l/G^2l)^{1/3}$.

4.3. Comparison between upflow and downflow data

In Fig. 6 the comparison of equation (2) with the data of Cumo *et al.* [4] in H-regime ($G = 503$ – 1043 kg/m² s, and $l/d = 256.4$) is also shown. It is noted that q_{c0} for upflow is about 11% higher than q_{c0} for downflow as in L-regime. The fact that the experimental data of q_{c0} lie a little lower than the prediction of equation (2) in Fig. 6 will be discussed later in Section 8.

4.4. Comparison with Freon-22 data

Figure 9 shows the comparison of equations (2) and (3) with q_c data derived through equations (6) and (8) from the experimental data of Freon-22 obtained by Staub (Table I and III) [21]. Though the column of q_c in Table I of [21] miscopies other data of CHF, q_c can be obtained from the data of $\Delta H_i/H_{fg}$ and χ_{ex} presented in the table via the heat balance [22]. Then, it may be noted in Fig. 9 that the data show a fairly good agreement with equation (2) except that some data lie a little lower than the prediction.

5. N-REGIME

5.1. Comparison with Freon-12 data

Groeneveld [5] made an experiment of Freon-12 in the region extending from negative to positive ΔH_i , and q_c at $\Delta H_i = 0$, that is q_{c0} , can be readily obtained from the reported $q_c - \Delta H_i$ relationship such as shown in Fig. 1, to give Fig. 10, where open symbols are the data in H-regime having the linear $q_c - \Delta H_i$ relationship (type A–A' in Fig. 1) while black symbols represent the data in N-regime having the non-linear $q_c - \Delta H_i$ relationship (type B–B' or B–B'' in Fig. 1). It is noted in Fig. 10 that the experimental data show a good agreement with the prediction of equations (2), (3) and (5).

5.2. Comparison with Freon-11 data

Purcupile *et al.* [23] have presented 37 data of Freon-11 ($l/d = 89.6$ and $p = 10.8$ – 24.8 bars), but it is found that all the data belong to N-regime without exception. Besides, the data fall in a very narrow range of ΔH_i , so that the direct comparison with equation (3) is impossible, because no correlation equation has yet been developed for the effect of subcooling in N-regime (cf. [10]). However, the imaginary quantity $(q_{c0}/GH_{fg})/(\rho_c/\rho_l)^{0.133}$, which can be derived through equations (6) and (8) from the above-mentioned data, is found to change accidentally in proportion to $(\sigma\rho_l/G^2l)^{0.15}$, so that the experimental value of $(q_{c0}/GH_{fg})/(\rho_c/\rho_l)^{0.133}$ at the boundary between N- and H-regime, for which $\sigma\rho_l/G^2l$ is determined by equation (5) for $l/d = 89.6$, can be readily extrapolated and the value thus

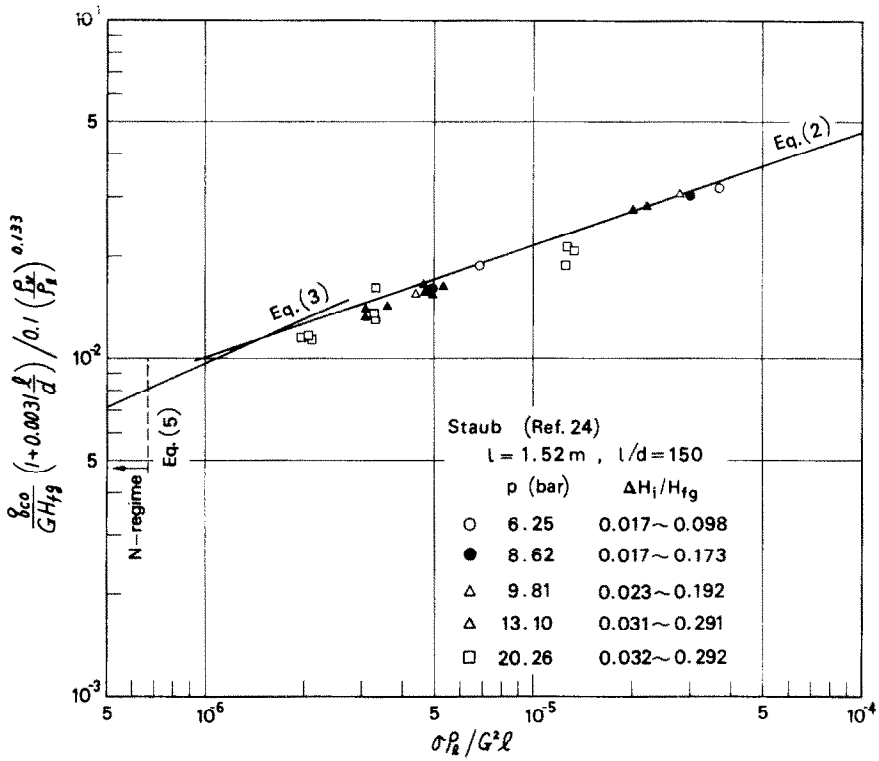


FIG. 9. Comparison between Freon-22 data in H-regime and the prediction of equations (2) and (3).

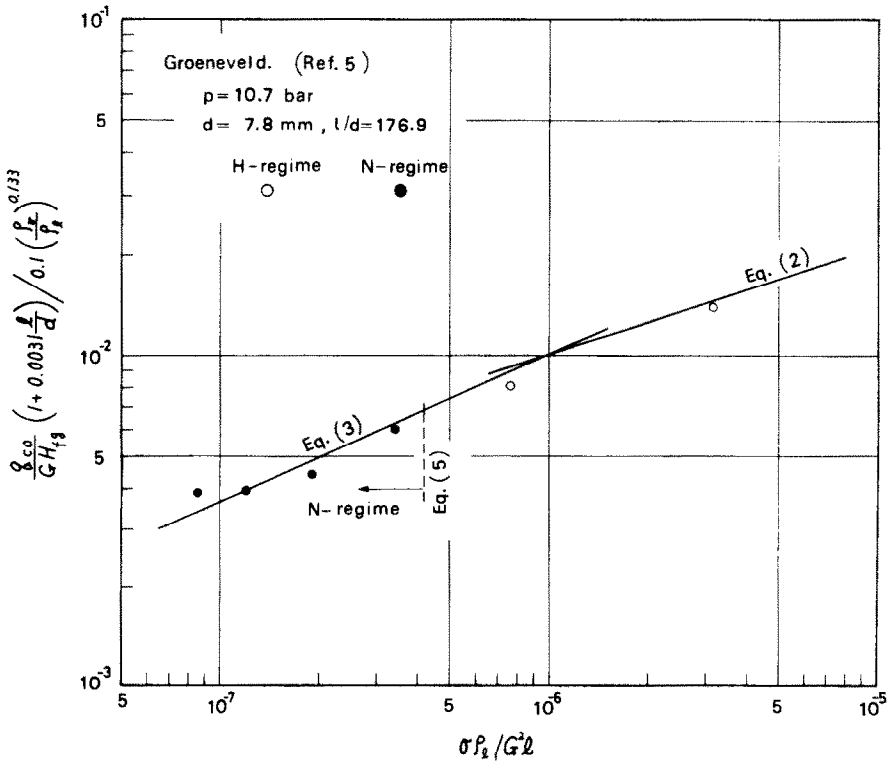


FIG. 10. Comparison between Freon-12 data in H- and N-regime and the prediction of equations (2), (3) and (5).

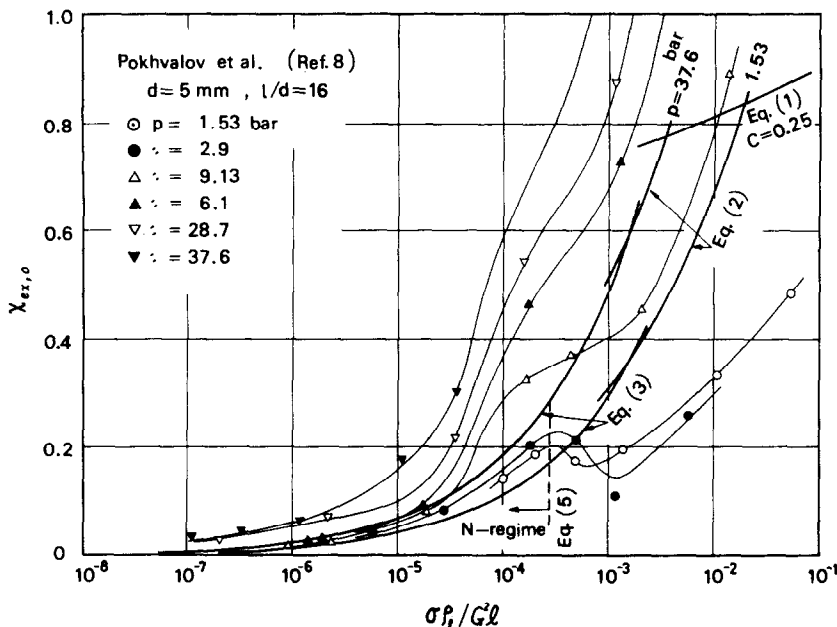


FIG. 11. Comparison between benzene data and the prediction of equations (1), (2), (3) and (5).

obtained is observed to agree well with the prediction of equation (3) at the above-mentioned boundary point.

5.3. Comparison with benzene data

Pokhvalov *et al.* [8] gave the experimental data of $q_{c,0}$ for benzene ($p = 1.53$ to 37.6 bars). In their experiment, not only is l/d very small as $l/d = 16$, but also it includes the range of very low mass velocities. Under such special conditions, natural convection boiling is apt to prevail rather than forced convection boiling (cf. VL-regime mentioned in the preceding study [10]); and in fact, Pokhvalov *et al.* themselves state that when mass velocity G is low, CHF shows the characteristics akin to those predicted by Kutateladze-Zuber correlation for CHF in pool boiling. According to Fig. 11, in which their experimental data are compared with equations (1)–(3) [transformed to $\chi_{ex,0}$ by equation (10)], it may be noticed that in the range of low G (that is, in the range of high $\sigma \rho_l / G^2 l$), natural convection boiling prevails as mentioned above so that the data show a great deviation from the prediction. However, as G is increased (that is, $\sigma \rho_l / G^2 l$ is reduced), the data in the range of $p = 1.53$ to 16.1 bars tend to show a good agreement with equation (3) in N-regime. As for the data in the range of higher pressure: $p = 28.7$ to 37.6 bars ($\rho_v / \rho_l = 0.14$ to 0.23), a slight deviation from equation (3) is observed, though the reason is unknown.

6. RELATIONSHIP OF $q_c - \Delta H_i$ IN THE RANGE OF $\Delta H_i < 0$

Exactly speaking, if the fluid fed to a tube has negative subcooling ($\Delta H_i < 0$) at inlet, it presents a problem that the two-phase flow at the inlet cannot be defined uniquely when only the value of ΔH_i is

specified. However, this problem will be left untouched here, and some information of $q_c - \Delta H_i$ relationship found in the analysis of experimental results will be noted below.

According to the experimental result of Cumo *et al.* [4], which has provided the result of Fig. 6, it may be permissible to say that in L- and H-regime, the linear $q_c - \Delta H_i$ relationship (type A–A' in Fig. 1) holds for $\Delta H_i < 0$ as well as for $0 < \Delta H_i$. This character is observed in the experiment of Groeneveld [5] too, but when $\sigma \rho_l / G^2 l$ is reduced so as to enter N-regime, the $q_c - \Delta H_i$ relationship of type B' in Fig. 1 begins to appear in the range of $\Delta H_i < 0$ keeping the onset of CHF at the tube exit, and as $\sigma \rho_l / G^2 l$ is reduced further, the $q_c - \Delta H_i$ relationship changes to the type B'' in Fig. 1 and at the same time the onset of upstream CHF appears.

7. TRANSITION BETWEEN H- AND HP-REGIME

Campolunghi *et al.* [6] reported the experiment of CHF of water for a vertical uniformly heated tube with a great length ($l = 11.25$ m, $d = 12$ mm) connected to an upstream, coiled preheating tube of the same length as above. The inlet subcooling ΔH_i of water entering the vertical tube is not given in their paper, but there is a statement that boiling occurs mainly in the vertical tube, so that $\Delta H_i = 0$ will be tentatively assumed here at the inlet of the vertical tube. The prediction of $\chi_{ex,0}$ obtained under this assumption from equations (2) and (4) [and equation (10)] is compared with the experimental data of Campolunghi *et al.* (given in Fig. 5 of [24]) in Fig. 12.

It may be observed in Fig. 12 that the agreement between the prediction of equation (4) and the data is comparatively good for HP-regime, whereas the data lie considerably higher than the prediction of

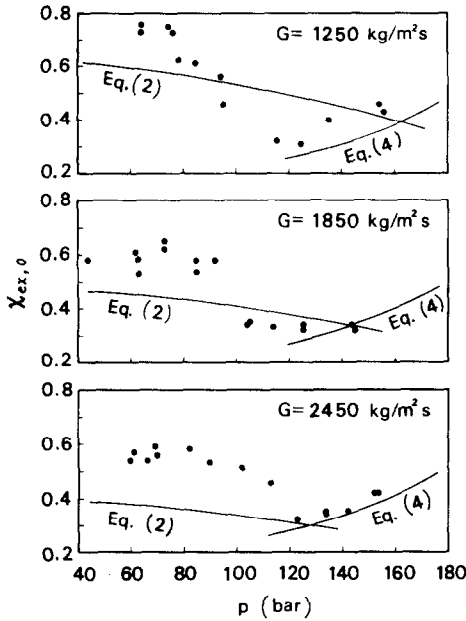


FIG. 12. CHF data of water obtained by Campolunghi *et al.* [6] for a very long, vertical tube ($l = 11.25$ m, $l/d = 937.5$).

equation (2) in H-regime. Taking into account the great length of tube ($l = 11.25$ m), the disagreement in H-regime may be attributed to the same cause as in the case of $l = 7.1$ m shown in Fig. 8. In addition, it should be noted that equations (2) and (4) can predict a rough trend for the transition between H- and HP-regime in Fig. 12, but it seems likely that further study is necessary for uncovering the more accurate feature of CHF in the vicinity of transition.

8. ON THE PROPRIETY OF DIMENSIONLESS GROUPS EMPLOYED

8.1. Prediction of mass flux scaling factor F_G

Apart from definite forms of correlation equations (1)–(9), let us only assume in this section that CHF in vertical uniformly heated round tubes is a phenomenon governed by five dimensionless groups q_c/GH_{fg} , $\sigma\rho_l/G^2l$, ρ_v/ρ_l , l/d , and $\Delta H_i/H_{fg}$. In this case, it follows that when the following conditions have been established between two different systems W and F :

$$(\rho_v/\rho_l)_W = (\rho_v/\rho_l)_F, \quad (l/d)_W = (l/d)_F, \quad (11)$$

and

$$(\Delta H_i/H_{fg})_W = (\Delta H_i/H_{fg})_F,$$

if the mass velocities $(G)_W$ and $(G)_F$ in the respective systems are selected so as to satisfy

$$(\sigma\rho_l/G^2l)_W = (\sigma\rho_l/G^2l)_F, \quad (12)$$

the following relation holds

$$(q_c/GH_{fg})_W = (q_c/GH_{fg})_F \quad (13)$$

so that $(q_c)_W$ in the system W can be known from the experimental data of $(q_c)_F$ in the system F . Now, if the case of $(d)_W = (d)_F$ is considered for simplicity, equation (13) can be rewritten under the condition of equations (11) and (12) as follows:

$$\frac{(q_c)_W}{(q_c)_F} = F_G \frac{(H_{fg})_W}{(H_{fg})_F}, \quad (14)$$

where

$$F_G = \frac{(G)_W}{(G)_F} = \left[\frac{(\sigma\rho_l)_W}{(\sigma\rho_l)_F} \right]^{1/2}.$$

Equation (14) is the prediction of mass velocity scaling factor F_G for the phenomenon controlled by the five dimensionless groups in equations (11)–(13).

8.2. Discussion

Regarding mass velocity scaling factor $F_G = (G)_W/(G)_F$, Dix [25] compared the experimental data of CHF obtained for Freons-114, -12, -22 and -21 with those for water to give the result that the empirical value of F_G thus obtained is in proportion to $[(\sigma\rho_v)_W/(\sigma\rho_v)_F]^{1/2}$. This result agrees with the prediction of equation (14) under the condition of $(\rho_v/\rho_l)_W = (\rho_v/\rho_l)_F$ given in equation (11).

On the other hand, Table 1 lists F_G given by equation (14) in case of $\rho_l/\rho_v = 20$ with the exception of $\rho_l/\rho_v = 590$ for water-potassium, together with the empirical values of F_G obtained by Stevens and Macbeth [26] for water-Freon-12, Staub [21] for water-Freon-22 and water-potassium, Coeffield [27] for water-Freon-113, and Hauptmann [28] for water-carbon dioxide. Table 1 also lists Ahmad's prediction of F_G [9], which is given by

$$F_G = \left[\frac{(\gamma/\rho_l\mu_l)_F}{(\gamma/\rho_l\mu_l)_W} \right]^{1/3} \left[\frac{(\mu_l/\mu_v)_F}{(\mu_l/\mu_v)_W} \right]^{1/8} \quad (15)$$

where $\gamma = |\partial(\rho_l/\rho_v)/\partial p|_{\text{sat}}$. It is noted in Table 1 that the prediction of equation (14) is always a little lower than the empirical value of F_G in case of Freons. On this point, it may not be useless to note the fact that statistically speaking, the experimental data of q_{c0} in

Table 1. Comparison of the value of F_G at density ratio $\rho_l/\rho_v = 20$ except $\rho_l/\rho_v = 590$ for water-potassium

System W	H ₂ O	H ₂ O	H ₂ O	H ₂ O	H ₂ O
System F	R-12	R-22	R-113	CO ₂	K
Equation (14)	1.28	1.34	1.21	1.19	1.24
F_G Empirical	1.40 [26]	1.40 [21]	1.46 [27]	1.13 [28]	~1.0 [21]
Ahmad [9]	1.38	1.38	1.34	1.2	1.1*

* The value for $\rho_l/\rho_v = 980$.

H- and N-regime have a trend to be somewhat lower than the prediction of equations (2) and (3) for Freons, which can be seen in Figs. 6 and 11 of the author's preceding study [10] as well as in Figs. 6 and 9 of the present study. On the contrary, Ahmad's prediction of F_G shown in Table 1 is much closer to the empirical value of F_G , and his prediction is primarily based on the framework having the following dimensionless group ψ_{CHF} instead of $\sigma\rho_l/G^2l$:

$$\frac{1}{\psi_{CHF}} = \left(\frac{\sigma\rho_l}{G^2d}\right)^{2/3} \left(\frac{Gd}{\mu_l}\right)^{1/3} \left(\frac{\mu_l}{\mu_v}\right)^{1/5} \quad (16)$$

This fact seems to imply that the viscosity of fluid can have the secondary effect on the occurrence of CHF of Freons in H- and N-regime at least. However, in order to give a definite answer to this problem, it may also be important to know more reliable data than those known at present for the surface tension of Freons. Besides, the deviation found between the prediction and the empirical value for water-potassium in Table 1 may be regarded to relate to a different cause, because it is concerned with the experimental data of potassium in L-regime shown in Fig. 5.

Finally, it may be of use to note that the propriety of the dimensionless group $\sigma\rho_l/G^2l$, which has not so far been taken into consideration in existing studies, cannot be examined here, because equation (12) is replaced by $(\sigma\rho_l/G^2d)_W = (\sigma\rho_l/G^2d)_F$ automatically under the condition $(l/d)_W = (l/d)_F$ given in equation (11).

8. CONCLUSIONS

(i) The generalized correlation [equations (1)–(9)], showing a fairly wide applicability, may be used as a tool for unifying independent experimental works of various kinds.

(ii) Tentative conclusions are given for CHF in L-regime as follows: usually, the constant C in equation (1) takes the value $C = 0.34$ for $\sigma\rho_l/G^2l < 5 \times 10^{-4}$ and $C = 0.25$ for $5 \times 10^{-4} < \sigma\rho_l/G^2l$ independently of the kind of fluid, and in the special case of very long tubes, CHF seems to be able to occur at the state of $\chi_{ex} = 1$.

(iii) Milan reproducibility tests data show a fairly good agreement with equations (1)–(3). In the special case of very long tubes, experimental data of CHF have a trend to deviate from equations (1)–(3) to some extent.

(iv) For fundamental investigations, the dimensionless groups with which the author's generalized correlation is composed have been examined through the comparison with the results of CHF modeling.

Acknowledgements—The financial support provided by the Ministry of Education is gratefully acknowledged, and also the author expresses his appreciation to Prof. K. M. Becker, Dr. K. Sanokawa and Mr. S. Yokoya for offering the important aid which is necessary for developing this study.

REFERENCES

1. Exercise on reproducibility of critical heat flux data, 1970 Meeting of the European Two-Phase Flow Group, June 8–11 (1970).
2. K. M. Becker, Burnout measurements in vertical round tubes, effect of diameter, TRM-RL-1260 (1970).
3. K. M. Becker and C. H. Ling, Burnout measurements in round tubes of 7100 mm heated length, KTH-NEL-13 (1970).
4. M. Cumo, R. Bertoni, R. Cipriani and G. Palazzi, Up-flow and down-flow burnout, in *Inst. Mech. Engrs Conference Publications 1977–8*, pp. 183–192 (1977).
5. D. C. Groeneveld, The occurrence of upstream dryout in uniformly heated channels, in *Proceedings of the 5th International Heat Transfer Conference*, Vol. 4 pp. 265–269. Hemisphere, Washington (1976).
6. F. Campolunghi, M. Cumo, G. Ferrari, R. Leo and G. Vaccaro, Burn-out power in once-through tubular system generators, in *Proceedings of the 5th International Heat Transfer Conference*, Vol. 4, pp. 280–284. Hemisphere, Washington (1974).
7. I. T. Arad'yev, I. G. Gorlov, L. D. Dodonov and O. S. Fedynskiy, Heat transfer to boiling potassium in uniformly heated tubes, *Heat Transfer—Soviet Res.* 1
8. Yu. Ye. Pokhvalov, I. V. Kronin and S. V. Yermakov, Critical heat fluxes in benzene boiling and saturation temperature, *Heat Transfer—Soviet Res.* 3(1), 23–29 (1971).
9. S. Y. Ahmad, Fluid to fluid modeling of critical heat flux: a compensated distortion model, *Int. J. Heat Mass Transfer* 16, 641–662 (1973).
10. Y. Katto, A Generalized Correlation of Critical Heat Flux for the Forced Convection Boiling in Vertical Uniformly Heated Round Tubes, *Int. J. Heat Mass Transfer* to be published.
11. A. W. Bennett, G. F. Hewitt, H. A. Kearsley, R. K. F. Keays and D. J. Pulling, Studies of burnout in boiling heat transfer, *Trans. Instn Chem. Engrs* 45, T319–T333 (1967).
12. P. B. Whalley, P. Hutchinson and G. F. Hewitt, The calculation of critical heat flux in forced convection boiling, in *Proceedings of the 5th International Heat Transfer Conference*, Vol. 4, pp. 290–294. Hemisphere, Washington (1974).
13. E. Nevstrueva, Different types of burnout in two-phase flow, in *JSME 1967 Semi-International Symposium Papers*, Vol. 2, pp. 35–43 (1967).
14. K. M. Becker, J. Bager and D. Djursing, Burnout correlations in simple geometries: most recent assessments, in *Seminar on Two-Phase Flow Thermohydraulics*, Rome, pp. 51–91 (June 9, 1972).
15. B. Thomson and R. V. Macbeth, Boiling water heat transfer burnout in uniformly heated round tubes: a compilation of world data with accurate correlations, AEEW-R 356 (1964).
16. J. P. Lewis, J. H. Goodykoontz and J. K. Kline, Boiling heat transfer to liquid hydrogen and nitrogen in forced flow, NASA TN D-1314 (1962).
17. G. F. Stevens, D. F. Elliott and R. W. Wood, An experimental investigation into forced convection burnout in Freon, with reference to burn-out in water, uniformly heated round tubes with vertical up-flow, AEEW-R 321 (1964).
18. P. G. Barnett and R. W. Wood, An experimental investigation to determine the scaling laws of forced convection boiling heat transfer, AEEW-R 443 (1965).
19. W. H. Lowdermilk, C. D. Lanzo and B. L. Siegel, Investigation of boiling burnout and flow stability for water flowing in tubes, NACA TN-4382 (1958).
20. A. A. Kiriyanenko, Experimental study of the surface tension of melts of alkali alloys by the combined method, *Heat Transfer—Soviet Res.* 4(1), 74–86 (1972).
21. F. W. Staub, Two-phase fluid modeling—the critical

- heat flux, *Nucl. Sci. Engng* **35**, 190–199 (1969).
22. F. W. Staub, Private communication.
 23. J. C. Purcupile, L. S. Tong and S. W. Gouse, Jr., Refrigerant—water scaling of critical heat flux in round tubes—subcooled forced-convection boiling, *J. Heat Transfer* **95**, 279–281 (1973).
 24. V. Marinelli, Critical heat flux: a review of recent publications, *Nucl. Technol.* **34**, 135–171 (1977).
 25. G. E. Dix, Freon—water modeling of CHF in round tubes, ASME-Paper No. 70-HT-26 (1970).
 26. G. F. Stevens and R. V. Macbeth, The use of Freon-12 to model forced convection burnout in water: the restriction on the size of the model, ASME-Paper No. 70-HT-20 (1970).
 27. R. D. Coefield, Jr., A subcooled DNB investigation of Freon-113 and its similarity to subcooled water DNB data, WCAP-7284 (1969).
 28. E. G. Hauptmann, V. Lee and D. W. MacAdams, Two-phase fluid modeling of the critical heat flux, in *Proceedings of the 3rd Canadian Congress on Applied Mechanics*, pp. 721–722. CANCAM, Calgary (1971). (4), 14–26 (1969).

UNE CORRELATION GENERALE DU FLUX THERMIQUE CRITIQUE EN
EBULLITION AVEC CONVECTION FORCEE DANS DES TUBES VERTICAUX
ET CHAUFFES UNIFORMEMENT. UN RAPPORT SUPPLEMENTAIRE

Résumé—On analyse les données de flux thermique critique (CHF) obtenues dans des études récentes incluant les tests de reproductibilité de Milan, en les comparant avec une corrélation générale qui a été développée par l'auteur dans une étude précédente. Non seulement de nouvelles informations sont obtenues sur la structure générale du CHF, mais on confirme aussi que la corrélation est valable en tant qu'outil pour unifier des expériences de divers types. La propriété des groupes adimensionnels qui composent la corrélation générale est testée en comparant les prévisions du facteur d'échelle du flux massique avec les valeurs empiriques obtenues sur le CHF.

EINE VERALLGEMEINERTE KORRELATION FÜR DIE KRITISCHE
WÄRMESTROMDICHTHE BEIM SIEDEN BEI ERZWUNGENER KONVEKTION
IN SENKRECHTEN, GLEICHMÄSSIG BEHEIZTEN, RUNDEN ROHREN
—ERGÄNZUNGSBERICHT

Zusammenfassung—Durch den Vergleich mit den Ergebnissen einer verallgemeinerten Korrelation, die vom Autor in der vorhergehenden Arbeit entwickelt wurde, wurden in dieser Arbeit vorliegende Daten über die kritische Wärmestromdichte analysiert. Diese Daten entstammen neuesten Untersuchungen, die die Reproduzierbarkeitstests von Milan und anderen beinhalten. Als Ergebnis wurden nicht nur neue Information über die allgemeine Struktur der kritischen Wärmestromdichte erhalten, sondern es wurde auch bestätigt, daß die obengenannte Korrelation ein brauchbares Instrument für die Vereinheitlichung von Untersuchungen der verschiedensten Arten ist. Außerdem wurde die Zweckmäßigkeit der dimensionslosen Gruppen, aus denen sich die verallgemeinerte Korrelation zusammensetzt, durch den Vergleich des berechneten Maßstabfaktors für den Massenstrom mit empirischen Werten geprüft, die man bei Modellversuchen zur kritischen Wärmestromdichte erhalten hat.

ОБОБЩЕННОЕ ВЫРАЖЕНИЕ ДЛЯ КРИТИЧЕСКОГО ТЕПЛООВОГО ПОТОКА
ПРИ КИПЕНИИ С ВЫНУЖДЕННОЙ КОНВЕКЦИЕЙ В ВЕРТИКАЛЬНЫХ РАВНОМЕРНО
НАГРЕВАЕМЫХ КРУГЛЫХ ТРУБАХ

Аннотация—С помощью обобщенного выражения, полученного автором в предыдущей работе, анализируются новые данные по критическому тепловому потоку (КТП). В результате анализа получены не только новые сведения о характере КТП, но и подтверждено, что предложенное выражение можно использовать для обобщения данных различных экспериментов. Кроме того, при сопоставлении результатов расчёта по обобщенному выражению и эмпирических значений, полученных при моделировании КТП, проверена корректность безразмерных комплексов, входящих в это выражение.